ALE-GAN: A 3D Conditional Generative Adversarial Network with Attention Learning Modules for Lung Nodule Segmentation

Manju Dabass[1], Anuj Chandalia[1], Suvrankar Datta[2], Dwarikanath Mahapatra[3]

[1]AI Research and Development Dept., Manentia AI Advisory Private Limited., India
[2]Radiodiagnosis & Interventional Radiology, AIIMS, India
[3]R&D Dept., Inception Institute of Artificial Intelligence, Abu Dhabi, UAE.

Abstract. Early lung cancer detection using lung nodule segmentation can enhance patient survival. In computer vision applications like medical image analysis, convolutional neural networks (CNN) outperform standard image processing methods. Convolutional neural network-based medical image segmentation methods have exhibited state-of-art performance, but they still face limitations. Data scarcity and class imbalance induce overfitting and poor performance. This study proposes a 3D conditional generative adversarial network implemented with scalar attention learning modules (Sc-ALM) for lung nodule segmentation that learns nodule-focused data distribution to boost accuracy. The proposed network utilizes Sc-ALM in generator part based on U-Net as well as the discriminator based on a simple classification network that empowered the model to distinguish ground truth from falsified segmentation. Also, Patch-based training reduces overfitting. The LUNA16 dataset is used to perform extensive lung nodule segmentation experiments. The proposed model's Boundary F1-score, average Jaccard Index, and Dice Similarity Coefficient are 0.9695, 0.9650, and 0.9825 respectively, outperforming various state-of-art models. This model has remarkable lung nodule segmentation performance and can help doctors diagnose lung nodules early by assessing their size, shape, and other properties.

Keywords: Deep Supervision, Attention Learning Mechanism, Generative Adversarial Network, Lung Nodule Segmentation.

1 Introduction

The worst ailments in the world, lung cancer poses a serious threat to humanity. According to GLOBOCAN 2020 [1], it has the highest fatality rate of 18% and the second-highest incidence rate of 11.4%. Lung cancer patients generally have a 21% five-year survival rate worldwide [2]. In India, 90% of lung cancer patients were diagnosed in advanced stages, which delayed treatment and decreased survival prospects, according to a study done in 2020 by Indian hospitals [3]. To improve patient survival

rates, it is necessary to find cancer early on. Patients who have long-lasting symptoms that are worsening, such as shortness of breath and hemoptysis (coughing up blood), should be screened for early-stage identification. Lung nodules, which range in size from 3 to 30 mm in the early stages, are lung lesions.

Additionally, lung lesions might be cancerous or benign. While malignant lung lesions are generally thought to be cancerous, benign lung lesions are typically thought to be non-cancerous. 95% of the time, nodules that are less than 14 mm in size are benign, while nodules that are more than 16 mm in size are malignant 84% of the time [4]. Considering that it can spread to other organs, a malignant lesion is more harmful. Therefore, early detection can help patients receive better care and stop the spread of cancer at the proper moment, increasing the likelihood that they will survive.

Segmenting lung nodules is essential for early-stage detection. According to [5], lung nodules can be categorized based on their location and relationships with neighboring structures, as well as their intensity profile. Lung nodules are divided into ground-glass and solid nodules based on the intensity profile. The ground glass nodules exhibit non-uniform intensity while solid nodules have a uniform intensity distribution. In addition, based on their position and connectivity with surrounding tissues, there are four different types of lung nodules: juxta-pleural nodules, nodules having pleural tail, well-circumscribed nodules, and juxta-vascular nodules. Patients with lung cancer are diagnosed via imaging tests such as Computed Tomography scans (CT), Positron Emission Tomography scans (PET), and X-rays. Although X-ray imaging is thought to be the primary diagnostic key step, the CT scan is often frequently employed after an X-ray reveals any worrisome areas. X-rays are used in CT imaging scans to record the three cross-sectional interpretation of the body component that must be examined in order to identify diseases. The axial, coronal, and sagittal cross-sectional view-based images are used to mark nodules in bounding boxes. As a result, CT scans can offer more precise information about the nodule's size and location. However, bronchoscopy or biopsy are preferred by clinicians [6] to determine the type of lung lesion. Medical image analysis allows us to offer a second viewpoint to medical professionals. Due to the high number of cancer patients, radiologists must analyze a vast volume of medical imaging data. However, there aren't too many radiologists in the world. For instance, in India, there is just one radiologist for every 100,000 patients [7]. Additionally, the number of CT and MRI imaging tests rises by an average of 7% annually while the number of radiologists increases by only 4%, according to the Clinical radiology UK workforce census 2020 report [8]. As a result, there is a significant workload on radiologists, which leads to deferred and error-prone diagnosis.

Deep learning-based methods and artificial intelligence (AI) have offered alternates for achieving lung nodule detection, segmentation, and classification. These methods have produced state-of-art performances for diverse computer vision applications, including those in the healthcare sector.

Following certain adjustments, the deep learning-based models have been tested for nodule identification and classification on lung CT images [9]. The [10] used attention learning based U-Net. Deep deconvolutional residual network, a U-Net variant-based method, is suggested in [12] for lung nodule segmentation. The authors offer a method for lung tumor segmentation based on a separable convolutional neural

network and construct a 2D-3D cascaded CNN methodology for lung nodule detection, segmentation, and classification in [13].

Highly precise object detection and semantic segmentation have been made possible by the development of region-based convolutional neural networks. These networks are made up of region proposal networks (RPNs), which generate various regions of interest (ROI) with objectness scores. A measurement of the interaction between object classes and backdrop is the objectness score. For the detection and segmentation of lung nodules, [14] offer a method based on Faster-RCNN and a fully convolutional neural network.

The drawback of region based CNNs is of their lesser adept at identifying areas with significant variance. Additionally, the size of lung nodules can range from a miniscule lesion having diameter of 3 mm to sizeable nodules having diameter of 30 mm. Cascaded Feature Pyramid Networks (FPNs) were used in [15] to detect various-sized lung nodules while accounting for multi-scale variance. The authors of [16] created a multi-view CNN for a comparable task, in which three separate views with various receptive fields—namely, 6×20×20, 6×30××30, and 6×40×40—were used to train three CNNs such that they can recognize nodules of various sizes.

To learn the features for training, supervised deep learning algorithms need a sizable amount of annotated data. There aren't many data, especially annotated data, in the field of medical imaging. As a result, several unsupervised algorithms are provided for the diagnosis of lung cancer as well as other tasks involving medical imaging. The ability of Generative Adversarial Network (GAN) based networks to learn data distribution without the use of annotation has recently made them prominent in the field of computer vision. However, the performance of GANs can be greatly enhanced by using annotations during training. In order to enhance segmentation outcomes for lung nodule segmentation, we offer a conditional GAN enabled with focused attention learning that is trained using ground truth segmentation masks.

Along with the data augmentation methods, GANs have recently shown to be important in image segmentation applications, particularly those for medical pictures. The segmentation map of the input picture is produced for the image segmentation task using the generator network of the GAN. The discriminator network modifies the weights of the entire network while attempting to differentiating the outputted and actual segmentation maps. As a consequence, training the generator and discriminator simultaneously can improve the segmentation outcomes. The [17] created a pix2pix (vox2vox) 3D version for segmenting brain tumours. The discriminator of this network was a classification network that determines whether the created segmentation map is true or fraudulent while generator was a segmentation network that generates the segmentation mask. Comparing the proposed network to the most advanced convolutional neural networks, remarkable results have been obtained.

The [18] developed a GAN-based strategy where conditional GAN is used for lung segmentation. The [19] suggest a technique based on transfer learning from a pre-trained model and using GAN. In order to more precisely learn the nodule features, the [20] model for lung nodule segmentation from CT images used an aggregation U-Net as the segmentation network for the generator. A classification network was then used in the discriminator to discriminate between the outputted segmentation and ground-truth masks. Compared to earlier methods, they had fantastic outcomes. Using

GANs, [21] described a method for segmenting lung nodules. They had optimized the network using SSSOA (Salp Shuffled Shepherd Optimization Algorithm).

Even though GANs offer cutting-edge performance in a variety of applications, they nevertheless have inherent limitations that can result in inadequate efficiency. Non-convergence and mode collapse are prevalent issues with GANs. Due to unstable training, the generator might collapse to generate a relatively smaller number of samples that are like one another. In order to help the discriminator learn effectively from real images, which can aid in the training and convergence of the model, some training improvement strategies are provided in [22]. One of these involves adding ground facts to the discriminator training. Another method that might help with the mode collapse problem is to provide the data in mini batches. In order to get more effective segmentation outcomes, our work leverages patch-based augmented images and ground-truth segmentation masks for improved training; and attention learning units for producing recalibrated features in the generator. Following are the study's main contributions:

- An attention learning enabled GAN-based technique has been proposed for segmenting lung nodules. Here, the generator is consisting of a segmentation network for separating the nodules and generating segmentation mask images for them. While the discriminator classifies real and fraudulent segmented nodule masks using a classification network.
- The scalar attention learning module (Sc-ALM) boost segmentation performance of the generator network while enhances the classification performance of the discriminator network in the proposed ALM-GAN.

The remainder of the paper is structured as follows: Section 2 describes the proposed approach; Section 3 details the experiments and outcomes; and Section 4 draws a conclusion.

2 Proposed method

In the proposed Attention Learning enabled GAN, generator is implemented as a segmentation network and discriminator is implemented as a classification network. For both the segmentation and classification network, we have introduced Scalar Attention Learning Modules (Sc-ALM) which helps in nodule specific feature recalibration across different scalar dimensions simultaneously. Due to this, segmentation as well as classification accuracy is enhanced. It is inspired by [23]. Fig. 1 is illustrating the detailed architecture of the proposed attention learning enabled GAN.

Figure 2 depicts the architectural network of the generator part, while Figure 3 depicts the architecture of the discriminator. In order to provide reference of actual labels to the generator and discriminator, the ground segmentation masks are introduced. To increase the accuracy of generator as well as discriminator, we conditioned the proposed GAN using the ground-truth labels. During training, the generator network uses ground truth as a reference and learns features from input patches. In order to discriminate between real and deceptive labels, the discriminator network is used. Both the discriminator and the generator use the back-propagation algorithm for training and updating the weights. We have applied a min-max

competition amongst discriminator and generator. Weights are updated as a result of the network loss function gradients being calculated using back-propagation.

2.1 **The Generator Network:** For the generator's segmentation network, we used a 3D adaptation of the U-Net [24] encoder-decoder structure with Sc-ALMs. Improved feature maps are produced as a result of these Attention learning modules that assists in recalibrated features across spatial as well as channel dimensions. Convolutional blocks make up the encoder portion. 3D convolution layers, batch normalisation, and ReLU activation functions are employed in each convolutional block. In the decoder section, there are up-sampling blocks made up of transposed convolutional, batch normalisation, and ReLU activation layers. The concurrent squeeze & excitation module is utilized at the terminal outcome of each block of the encoder as well as decoder to recalibrate the features and capture just the pertinent features. The generator network receives 3D patches with an input size of 64 by 64 by 32 and generates a final segmentation mask that is further sent as one of the inputs to the discriminator.

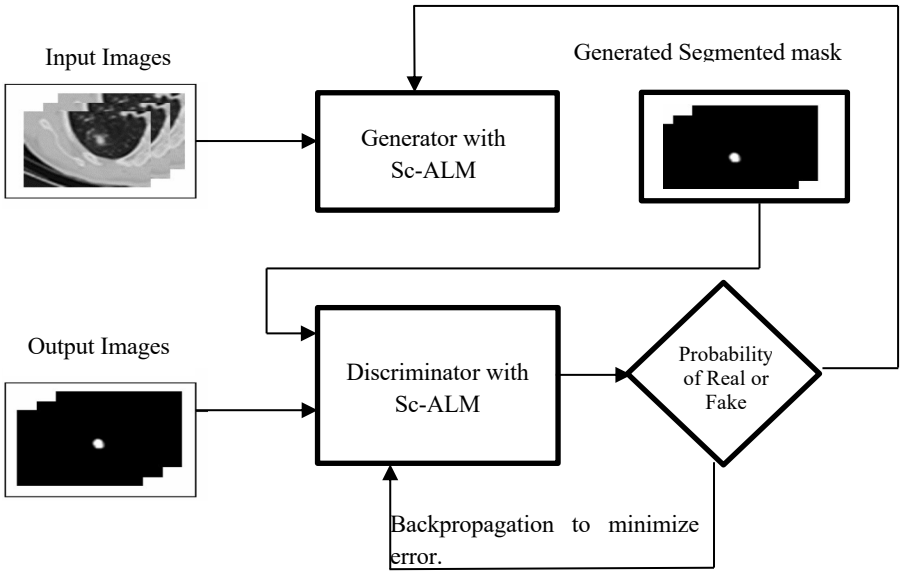

Fig. 1. Structure of the proposed attention learning enabled GAN

2.2 **Discriminator:** For the discriminator network, we have constructed a classification network made up of convolutional blocks, dense blocks, and Attention Learning Modules. A set of the globally distributed channel-wise features is created in the scalar attention learning module after feature recalibration is carried out throughout the channel dimension. This boosts the performance of categorization by enhancing the quality of feature representations. The attention learning module was therefore added to the discriminator. Each convolutional block has a batch normalisation step, a Leaky-ReLU activation function, and three 3D convolution layers. Prior to the implementation of the last dense layer with sigmoid function, a ReLU activation function layer is included in the dense block. The segmented nodule masks from the ground truth and the segmented nodule mask outcomes of the generator network are the discriminator's two inputs. The outcome produced by the discriminator network is the form of probability index of original and counterfeit segmentation masks. Using discriminator loss, the accuracy of the generator for providing accurate segmentation masks increases.

2.3 **Scalar Attention Learning Module (Sc-ALM):** The Scalar Attention Learning Module (Sc-ALM) has been introduced as a way of enhancing the proposed classification model's potential of focus-refinement. It allows the GAN design to understand how to use universal channels and scalar information to prioritize the nodule-specific features. It exploits the scale dependencies while performing adaptive recalibration of channel-specific features generated via related network, and it identifies the scale for which these generated channel-specific weighted feature maps are utmost beneficial for the chosen task. Fig. 1 demonstrates this.

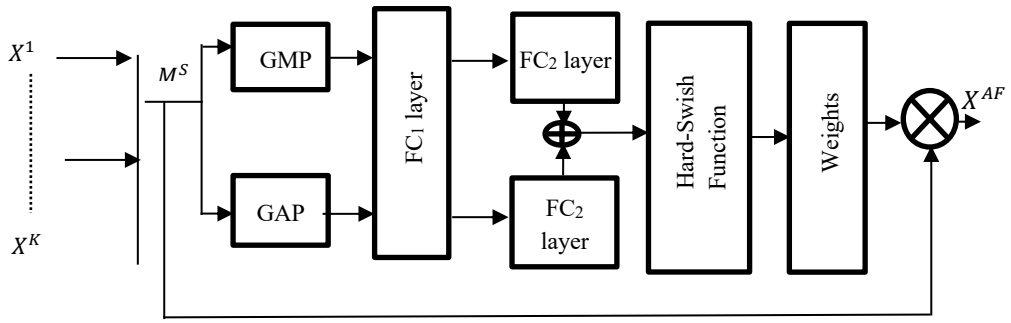

Fig. 2. Components of Scalar Attention Learning Module (Sc-ALM)

The Sc-ALM renders more efficient usage of the extracted features by leveraging the scalar dependences to establish the scales for which these attention-weighted feature maps have a significant influence on the classification of a certain class. The M^O inputted to the Sc-ALM is contingent on the outcomes obtained from the generator or discriminator network. Since max-pooling and average pooling are considered to complement each other in capturing multi-scalar information [25], both functions efficiently together. Consequently, to aggregate M^O in this case, global max-pooling

i.e., GMP and global average pooling i.e., GAP are used. It results in two global descriptors G_{max}^{O} and G_{avg}^{O}. These global descriptors are then concatenated. For learning the non-linear interactions amongst diverse scales, these two descriptors are inputted to two mutual Fully Convolutional (FC) layers and their subsequent results are fused via elemental summation, trailed by the Hard-Swish activation function.

3 Experiments and results

3.1 Dataset

The publicly accessible LUNA16 dataset given at [26] was used for the present study. In this dataset, the extensive scans are processed using a separate metric. Because lung nodules might be rather minute, it is necessary to choose a thin slice in order to identify them. There are 888 CT scans after omitting scans having slice thickness greater than 2.5 mm for this reason. Scanners that have erratic slice spacing or missing slices are also eliminated. Following this procedure, a dataset of 888 CT scans accompanied by 36,378 radiologists' annotations was created. The resulting dataset was made available in the LUNA16 challenge, where only those annotations that were categorized as nodules (3 mm) were thought to be significant while the other annotations that either contained nodules smaller than 3 mm in size or non-nodules were not thought to be substantial for lung cancer screening protocol.

3.2 Data pre-processing

For a Lung Cancer patient, the CT scans are imbibed with three distinct views i.e., Sagittal, Axial, and Coronal planes for lung imaging. Furthermore, Hounsfield Units (HU) ranging (-1000,1000) are used to assess radio-density in CT scans for the lung nodule segmentation task is. In order to get the appropriate HU range, we first transformed the data. In all datasets, a CT image slice's initial dimensions are 512 x 512. Depending on the CT scanner's resolution, each case requires a different number of slices. Using the patchify package, we extracted random 3D patches with dimensions of 64 x 64 x 32 from the CT scans. A patch with the dimensions 64 x 64 x 32 has 64 for the patch's height and width and 32 for its subsequent slice number. The patch size is to 64 x 64 x 32 and the step size to 32 for extracting patches. The patch size of 64 x 64 x 32 is chosen to amply encompass the nodules having the largest diameter along with a slice quantity of 32 as the number of total slices needed to study a nodule with a diameter between 3 and 30 mm varies between 3 and 30, roughly.

3.3 Loss Function

As the proposed attention learning enabled GAN is consisting of a generator-discriminator network, the adversarial loss function utilized by the conditional GAN given by

$$L_C\ (G, D) = E_{X \sim P_D}[\log P(X|t)] + E_{G(Y) \sim P_G}[\log 1 - P(G(Z|t))] \quad (1)$$

where P_D is representing the data dissemination while X illustrates the real sample quantity. $P(X)$ signifying the probability of the true samples that are categorized as

true. P_G is depicting the model dissemination while the samples spawned are described by $G(\mathrm{Z})$. Thus, $P(\mathrm{G}(\mathrm{Z}))$ is the probability of the produced samples being categorized as original. The generator G attempts to minimize the adversarial loss i.e., $P(\mathrm{G}(\mathrm{Z}))$ closer to 1 by providing generated samples as much as closer to the real samples, and the discriminator P attempts to maximize the adversarial loss by making the value of $\mathrm{P}(\mathrm{G}(\mathrm{Z}))$ closer to zero.

Also utilized was the dice loss in the generator for performing weight updation throughout training. It is given by:

$$L_{DICE}(G) = 1 - \frac{2TP}{2TP+FP+FN} \tag{2}$$

Thus, the absolute loss becomes can be depicted by

$$L_{ALE-GAN}(G, D) = L_C(g, D) + L_{DICE}(G) \tag{3}$$

Therefore, the final objective of the proposed ALM-GAN for accurately segmenting the lung nodules is given by:

$$Objective\_Function = \min_G \max_D L_{ALM-GAN}(G, D) \tag{4}$$

3.4 Training

We have employed 620 CT scan images for training, 180 CT scan images for validation, and the final 88 CT scan images for testing the proposed approach out of a total of 888 scans. The training imaging data size is increased by using patch-based augmentation technique. The input patch size is chosen as 64×64×32, and there is only one channel. For training the model with the deep learning-based frameworks of Tensorflow version 1.14 and Keras version 2.2.4, we used a 16 GB NVIDIA P100 GPU with 128 GB RAM, cuDNN 7.4, and CUDA 10.0. The weights of the discriminator and generator layers are updated using the adversarial loss function and dice loss. The discriminator and generator are optimized through employ of the Adam optimizer.

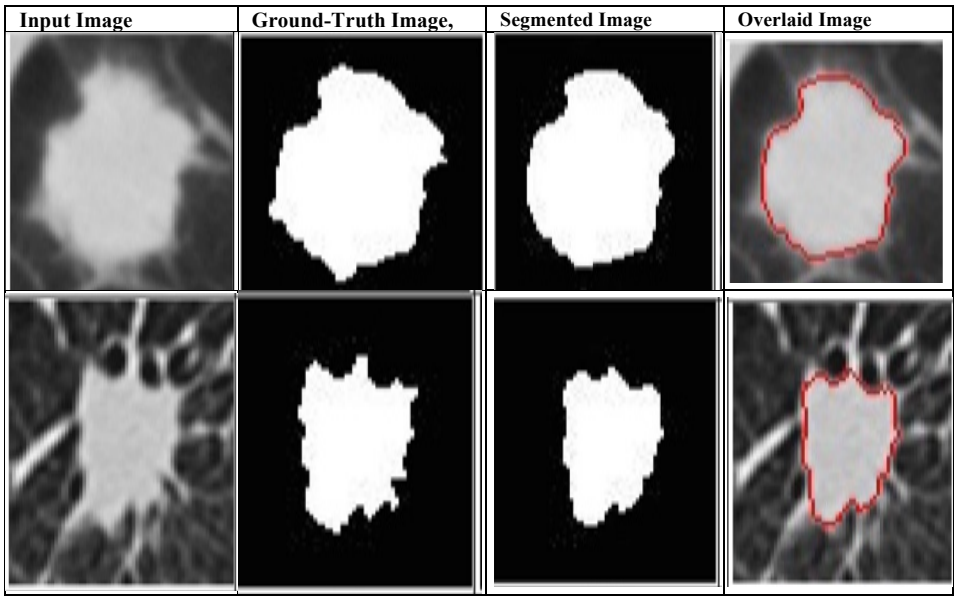

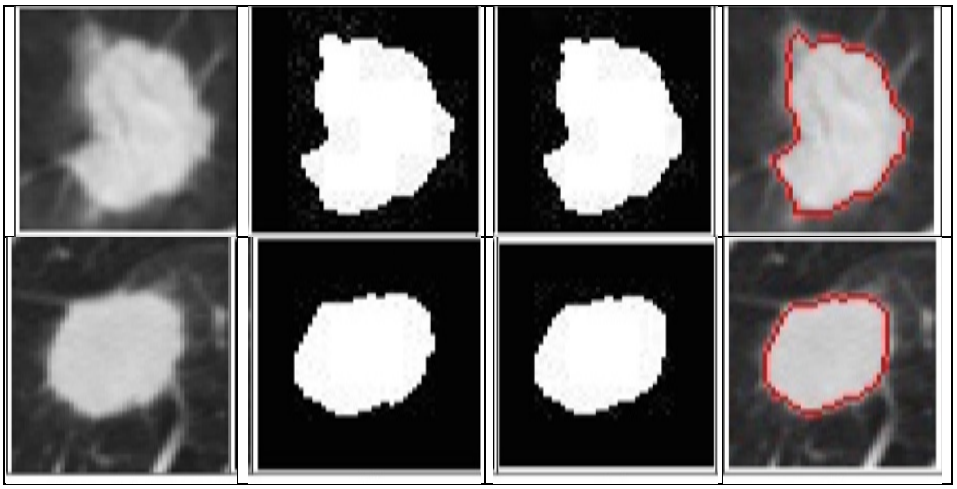

Fig. 3. Nodule Segmentation Experimental Outcomes:

3.5 Evaluation Metrics

Six quantitative analysis metrics: Accuracy (Acc), Sensitivity (Sen), Dice Similarity Coefficient (DSC), Specificity (Spec), Jaccard Index (JI), and Boundary F1-Score are computed here to examine the nodule segmentation outcomes.

3.6 Segmentation results

The segmentation outcomes of the proposed attention learning enabled GAN is displayed in Fig. 3 utilizing four different scenarios. The findings demonstrate how closely the predicted segmentation masks resemble the actual segmentation masks. The segmentation results show that the proposed network successfully segments nodules of different sizes.

3.7 Comparative analysis

The comparison of our proposed ALE-GAN with the recently proposed methodologies is enumerated in Table 1. It is clearly depicted from this table that our proposed approach is able to attain enhanced performances than the other state-of-the-art methodologies.

Table 1. Performance comparison results of the State-of-Art models

Techniques	Year	Applied Methodology	DSC Score
[26]	2019	A deep fully convolutional network	93.00
[27]	2020	A semi-automated 3-D deep residual U-Net	87.50
[19]	2020	Aggregation-U-net GAN (AUGAN) system	85.40
[28]	2020	3D-unet Neural Network	95.30

[29]	2021	GAN based Deep learning model with Salp Shuffled Shepherd Optimization	79.86
[18]	2021	GAN and transfer learning	72.7
[20]	2021	SSSOA-GAN	79.86
[30]	2022	U-Net architecture-based DL model	80.74
[31]	2022	DENSE-UNET	74.42
Proposed	**2023**	**ALE-GAN**	**97.15**

4. Conclusion

Nodule segmentation is a fundamental and critical step in the early recognition of lung cancer. Here, an attempt is made to help the radiologists by offering a second opinion. The Sc-ALMs are applied in the generator and discriminator networks to develop proposed attention learning enabled GAN specifically focused for lung nodule segmentation task. The patch-based augmentation is employed as data pre-processing. The publicly accessible dataset given for the LUNA16 challenge is applied to train, test, and validate the proposed network. It has been noted that patch-based processing aids in boosting the training dataset's sample size, which resolves the issues of data scarcity and model overfitting. The network's computation complexity is decreased as a result of the small size of the patches. Additionally, patch-based model training increases the network's ability to acquire imperative characteristics of lung nodules. Sc-ALMs in the network also make it more resilient since they can concentrate on the pertinent data. Consequently, our proposed network performed significantly well with a dice similarity coefficient score of 97.15.

References

[1] J. Ferlay, M. Colombet, I. Soerjomataram, D.M. Parkin, M. Piñeros, A. Znaor, F. Bray, Cancer statistics for the year 2020: An overview, Int. J Cancer 149 (4) (2021) 778–789.

[2] R.L. Siegel, K.D. Miller, H.E. Fuchs, A. Jemal, Cancer statistics, 2021, CA: Cancer J. Clin. 71 (1) (2021) 7–33.

[3] P. Mathur, K. Sathishkumar, M. Chaturvedi, P. Das, K.L. Sudarshan, S. Santhappan, V. Nallasamy, A. John, S. Narasimhan, F.S. Roselind, et al., Cancer statistics, 2020: report from national cancer registry programme, India, JCO Glob. Oncol. 6 (2020) 1063–1075.

[4] G.A. Silvestri, N.T. Tanner, P. Kearney, A. Vachani, P.P. Massion, A. Porter, S.C. Springmeyer, K.C. Fang, D. Midthun, P.J. Mazzone, et al., Assessment of plasma proteomics biomarker's ability to distinguish benign from malignant lung nodules: results of the PANOPTIC (Pulmonary Nodule Plasma Proteomic Classifier) trial, Chest 154 (3) (2018) 491–500.

[5] A.K. Dhara, S. Mukhopadhyay, N. Khandelwal, Computer-aided detection and analysis of pulmonary nodule from CT images: A survey, IETE Tech. Rev. 29 (4) (2012) 265–275.

[6] S.N. Lavasani, P. Farnia, E. Najafzadeh, S. Saghatchi, M. Samavati, H. Abtahi, M. Deevband, A. Ahmadian, Bronchoscope motion tracking using centerline-guided Gaussian mixture model in navigated bronchoscopy, Phys. Med. Biol. 66 (2) (2021) 025001.

[7] R. Arora, The training and practice of radiology in India: current trends, Quant. Imaging Med. Surg. 4 (6) (2014) 449.

[8] R C of Radiologists, Clinical radiology uk workforce census 2020 report, 2021, URL https://www.rcr.ac.uk/publication/clinical-radiology-uk-workforce-census2020-report.

[9] H. Xie, D. Yang, N. Sun, Z. Chen, Y. Zhang, Automated pulmonary nodule detection in CT images using deep convolutional neural networks, Pattern Recognit. 85 (2019) 109–119.

[10] Dabass, M., Chandalia, A., Gupta, H. & Senasi, R., 2023, May. Lung Segmentation in CT scans with Residual Convolutional and Attention Learning-based U-Net. In 2023 International Conference on Recent Advances in Electrical, Electronics & Digital Healthcare Technologies (REEDCON) (pp. 240-245). IEEE.

[11] G. Singadkar, A. Mahajan, M. Thakur, S. Talbar, Deep deconvolutional residual network based automatic lung nodule segmentation, J. Digit. Imaging 33 (3) (2020) 678–684.

[12] P. Dutande, U. Baid, S. Talbar, LNCDS: A 2D-3D cascaded CNN approach for lung nodule classification, detection and segmentation, Biomed. Signal Process. Control 67 (2021) 102527.

[13] X. Huang, W. Sun, T.-L.B. Tseng, C. Li, W. Qian, Fast and fully-automated detection and segmentation of pulmonary nodules in thoracic CT scans using deep convolutional neural networks, Comput. Med. Imaging Graph. 74 (2019) 25–36.

[14] Y. Xiao, X. Wang, Q. Li, R. Fan, R. Chen, Y. Shao, Y. Chen, Y. Gao, A. Liu, L. Chen, et al., A cascade and heterogeneous neural network for CT pulmonary nodule detection and its evaluation on both phantom and patient data, Comput. Med. Imaging Graph. 90 (2021) 101889.

[15] M.M.N. Abid, T. Zia, M. Ghafoor, D. Windridge, Multi-view convolutional recurrent neural networks for lung cancer nodule identification, Neurocomputing (2021).

[16] M.D. Cirillo, D. Abramian, A. Eklund, Vox2Vox: 3D-GAN for brain tumour segmentation, 2020, arXiv preprint arXiv:2003.13653.

[17] S.P. Pawar, S.N. Talbar, LungSeg-Net: Lung field segmentation using generative adversarial network, Biomed. Signal Process. Control 64 (2021) 102296.

[18] M. Nishio, K. Fujimoto, H. Matsuo, C. Muramatsu, R. Sakamoto, H. Fujita, Lung cancer segmentation with transfer learning: usefulness of a pretrained model constructed from an artificial dataset generated using a generative adversarial network, Front. Artif. Intell. (2021) 95.

[19] Z. Shi, Q. Hu, Y. Yue, Z. Wang, O.M.S. AL-Othmani, H. Li, Automatic nodule segmentation method for CT images using aggregation-u-net generative adversarial networks, Sens. Imaging 21 (1) (2020) 1–16.

[20] S. Jain, S. Indora, D.K. Atal, Lung nodule segmentation using salp shuffled shepherd optimization algorithm-based generative adversarial network, Comput. Biol. Med. 137 (2021) 104811.

[21] T. Salimans, I. Goodfellow, W. Zaremba, V. Cheung, A. Radford, X. Chen, Improved techniques for training gans, Adv. Neural Inf. Process. Syst. 29 (2016) 2234–2242.

[22] A.G. Roy, N. Navab, C. Wachinger, Concurrent spatial and channel 'squeeze & excitation'in fully convolutional networks, in: International Conference on Medical Image Computing and Computer-Assisted Intervention, Springer, 2018, pp. 421–429.

[23] M. Dabass, and J. Dabass. An Atrous Convolved Hybrid Seg-Net Model with residual and attention mechanism for gland detection and segmentation in histopathological images. Computers in Biology and Medicine 155 (2023): 106690.

[24] M. Dabass, S. Vashisth, and R. Vig. A convolution neural network with multi-level convolutional and attention learning for classification of cancer grades and tissue structures in colon histopathological images. Computers in biology and medicine 147 (2022): 105680.

[25] M. Dabass, J. Dabass, S. Vashisth, and R. Vig. A hybrid U-Net model with attention and advanced convolutional learning modules for simultaneous gland segmentation and cancer grade prediction in colorectal histopathological images. Intelligence-Based Medicine 7 (2023): 100094.

[26] LUNA16, LUNA16 challenge dataset available, 2016, (online), https://luna16. grand-challenge.org/download/, (Accessed 21 October 2021).

[27] U. Baid, S. Talbar, S. Rane, S. Gupta, M.H. Thakur, A. Moiyadi, N. Sable, M. Akolkar, A. Mahajan, A novel approach for fully automatic intra-tumor segmentation with 3D U-net architecture for gliomas, Front. Comput. Neurosci. 14 (2020) 10.

[28] Roy, R., Chakraborti, T., & Chowdhury, A. S. (2019). A deep learning-shape driven level set synergism for pulmonary nodule segmentation. Pattern Recognition Letters, 123, 31-38.

[29] Usman, M., Lee, B. D., Byon, S. S., Kim, S. H., Lee, B. I., & Shin, Y. G. (2020). Volumetric lung nodule segmentation using adaptive roi with multi-view residual learning. Scientific Reports, 10(1), 12839.

[30] Xiao, Z., Liu, B., Geng, L., Zhang, F., & Liu, Y. (2020). Segmentation of lung nodules using improved 3D-UNet neural network. Symmetry, 12(11), 1787.

[31] Jain, S., Indora, S., & Atal, D. K. (2021). Lung nodule segmentation using salp shuffled shepherd optimization algorithm-based generative adversarial network. Computers in Biology and Medicine, 137, 104811.

[32] Lu, D., Chu, J., Zhao, R., Zhang, Y., & Tian, G. (2022). A Novel Deep Learning Network and Its Application for Pulmonary Nodule Segmentation. Computational Intelligence and Neuroscience, 2022.